Heterogeneous Visible Light and Radio Communication for Improving Safety Message Dissemination at Road Intersection

Gurinder Singh, Anand Srivastava, Vivek Ashok Bohara, Zilong Liu, Md Noor-A-Rahim and Gourab Ghatak

Abstract—Visible light communication (VLC) has recently emerged as an affordable and scalable technology supporting very high data rates for short range vehicle-to-vehicle (V2V) communication. In this work, we advocate the use of vehicular-VLC (V-VLC) for basic safety messages (BSMs) dissemination in lieu of conventional vehicular radio frequency (V-RF) communication in road intersection applications, where the reception performance is affected by interference from the concurrent transmissions of other vehicles. We make use of stochastic geometry to characterize the interference from the same lane as well as the perpendicular lane for various network configurations, i.e., standalone V-VLC, stand-alone V-RF and hybrid V-VLC/V-RF network. Specifically, by modelling the interfering vehicles' locations as a spatial Poisson point process (PPP), we are able to capture a static two-dimensional road geometry as well as the impact of interference due to vehicles clustering in the vicinity of road intersection in terms of outage probability and throughput. In addition to above, the performance of spatial ALOHA and carrier sense multiple access with collision avoidance medium access control (CSMA/CA MAC) protocol for standalone V-VLC, standalone V-RF and hybrid V-VLC/V-RF network configuration for relaying BSMs at road intersection is also compared. The performance metrics such as delay outage rate (DOR) and information outage rate (IOR) are utilized to investigate the impact of latency associated with various network configurations. Our numerical results reveal that our proposed hybrid V-VLC/V-RF leads to significant improvement in terms of outage performance, throughput and latency as compared to stand-alone V-VLC or stand-alone V-RF network.

Index Terms—Stochastic geometry, Visible Light Communications (VLC) based V2X, Hybrid V-VLC/V-RF network.

I. INTRODUCTION

RECENTLY, vehicle-to-everything (V2X) networks have gained considerable attention as an integral component of future intelligent transportation system (ITS) for facilitating communications between vehicle-to-vehicle (V2V) and vehicle to-roadside units (V2RSU) networks [1]. Dedicated short-range communication (DSRC), which is a key component of V2X network to enhance the road safety, forms an important part of the IEEE 802.11p standard [2]. The vehicular-radio frequency (V-RF) communication tends to suffer from higher interference, longer communication delays, and lower packet

Gurinder Singh, Anand Srivastava, Vivek Ashok Bohara, and Gourab Ghatak are with the Department of Electronics and Communications Engineering, IIIT-Delhi, New Delhi, India (E-mail: {gurinders, anand, vivek.b, gourab.ghatak}@iiitd.ac.in). Zilong Liu is with the School of Computer Science and Electronic Engineering, University of Essex, UK (E-mail: zilong.liu@essex.ac.uk). Md Noor-A-Rahim is with the School of Computer Science & IT, University College Cork, Ireland (E-mail: m.rahim@cs.ucc.ie).

delivery rates as the density of the vehicles increases. To improve the reaction time in critical scenarios and to obtain full situational awareness, one requires relatively long communication ranges, extremely low latencies (typically below 50 ms in pre-crash situations), as well as high packet delivery ratios [3], [4]. These requirements in combination with a possible high traffic density, constant topology changes as well as rapidly changing signal propagation conditions makes the design of vehicular communication network very challenging. In current scenario, the impact of V2X communications on the amount of utilized RF spectrum is low, however it is expected to significantly increase in the near future. The existing RF bands allocated for V2X communication can quickly suffer from considerable interference when large number of vehicles located in the same vicinity try to communicate simultaneously. In last few years or so, researchers have proposed numerous solutions to address this potential bandwidth congestion problem. One such possible solution is to employ visible light communication (VLC) for vehicular scenario.

VLC is considered as a complementary potential candidate for future optical wireless communication due to the increase in deployment of LED and existing lighting infrastructure [5], [6]. The inherent features of VLC such as low power consumption, wide free spectrum, enhanced security, and anti-electromagnetic interference makes it an ideal candidate for future intelligent transportation system (ITS). The vehicular-visible light communication (V-VLC) may be implemented by using the existing LEDs in vehicle headlamps and taillight. Despite all the aforementioned VLC advantages, VLC also suffers from the fact that most of its applications are mainly based on line-of-sight (LOS) components. Therefore, recent literature has focused on the feasibility of integrating this technology with the existing DSRC to improve the performance of the V2X networks. In particular, V-RF and V-VLC can be used as complementary technology for V2X networks. For instance, V-RF based technology may be appropriate for long range communication, whereas V-VLC based technology may be suitable for high traffic density scenarios. The co-deployment of V-RF and V-VLC technology may significantly improve the overall performance of V2X network in terms of reliability and low latency.

Road safety is a major issue, and more importantly at accident prone scenarios (eg road intersections, crossroads etc). V2X communication offer several applications related to accident prevention, such as sending basic safety messages (BSMs)/ cooperative awareness messages (CAMs) that alert

vehicles about accidents happening in their surrounding. One of the major drawbacks that effect V2X communication is interference. Hence, investigating the performance of V2X network in the presence of interference is crucial for designing safety applications at urban as well as suburban intersections. At road intersection, we need to relay the BSMs/CAMs, as V2V communications may be obstructed by the buildings. A well-known solution is relaying with the assistance of RSU. However, the packet reception probability at RSU may be heavily impacted due to interference caused from concurrent transmission. Therefore, if the packet reception probability at RSU is low, the relaying performance will also be low. One solution is to use sector antennas at the RSU which is however not a cost effective solution. Alternatively, one can design VLC based vehicle-to-infrastructure (V2I) communication where the RSU integrated on road lamp or traffic light can receive/transmit BSM through VLC. However, still there exists challenges associated with feasibility of standalone V-VLC and standalone V-RF network. In this paper, we compare the performance of standalone V-VLC, standalone V-RF and propose a hybrid V-VLC/ V-RF framework, specifically for intersection scenarios. We provide an analytical framework to characterize interference for various network configurations using various analytical tools of stochastic geometry.

A. Literature Review

Conventional vehicular ad hoc networks (VANETs) utilizes RF for V2V communications [7], [8]. Since RF links are less likely to be blocked entirely by obstacles, vehicles can communicate with appreciably large transmission range. However, this could also potentially lead to a wide interfering coverage area. For example, an RF network may experience enormous interference incurred by high-density traffic [9], which may result in reduced network efficiency [10]. Apart from the above, a limited RF bandwidth could also constrain the network performance [10]. Lately, VLC has been shown as an effective means to overcome these issues in both indoor and outdoor scenarios [11]. The superiority of VLC over conventional RF is due to the following reasons: 1) it makes use of LEDs which are cheap, ubiquitous in all modern vehicles, street lamps and digital signage, as well as it has high power efficiency; 2) no licensing fee required; 3) end-to-end secure data transmission rates and high spatial reuse ratio; 4) interference-free with the existing RF networks due to the fact that light operates in a different spectrum band [12], [13]. Nevertheless, many recent studies have recognized the critical drawbacks of employing the stand-alone VLC in V2V communications. Note that VLC is fundamentally based on the line-of-sight (LOS) communication. There is an increased chances of connectivity loss for VLC based vehicular network [14]. In order to address these issues, researchers have proposed hybrid RF/VLC systems [15]–[18], where end users can benefit the wide coverage area provided by RF systems and the large data rates from VLC systems. Such hybrid networks are practically feasible, as RF and VLC systems can coexist without causing much interference on each other and can operate in the same environment. Comparing hybrid RF/VLC

systems with systems that employ either stand-alone RF or VLC only, the authors in [19]–[21] demonstrated a noticeable increase in data transmission energy efficiency, delay and throughput performance for an indoor environment. As far as an outdoor environment is concerned, the authors in [22] studied a point-to-point (P2P) transmission scenario in which the system can switch between either RF links or VLC links after analyzing the SNR ratio levels in each link.

Stochastic geometry is an effective means to characterize the randomness in the location of vehicles [23]. Recent works such as [24] and [25] characterize the interference in RF networks where the signal-to-interference ratio (SIR) and the average network throughput are estimated. The authors in [26] and [27] applied stochastic geometry in vehicular ad-hoc networks (VANET) to determine the probability of successful transmission while assuming that road vehicles are spatially distributed according to a linear Poisson point process (PPP). More often, the 1D PPP model is more relevant for VANETs [26]. For these vehicular scenarios, clustering has been addressed in [28], while effects due to the 802.11p carrier sense multiple access (CSMA) MAC protocol have been investigated in [29], [30], [31]. It is noted that while these works enable communication system design for one-dimensional highway scenarios, they do not capture well the salient effects of intersections. The latter has been briefly studied in [32], [33], indicating that it is important to properly model interference from different roads and take into account the clustering of vehicles close to the intersection.

To the best of authors' knowledge, so far, not sufficient literature is available which provides comprehensive framework for performance study and comparison of standalone V-VLC, standalone V-RF and hybrid V-VLC/V-RF network configuration using analytical tools such as stochastic geometry. We intend to propose the benefits of employing hybrid V-VLC/V-RF network over standalone V-VLC or V-RF network in terms of outage performance and throughput. Also, we intend to show the latency associated with various network configurations for relaying BSMs at road intersection in terms of data oriented characterization viz. delay outage rate (DOR) and information outage rate (IOR).

B. Contribution

A primary objective of this work is to showcase the potential benefit of employing V-VLC along with conventional V-RF by improving the relaying performance of BSMs at road intersections.

Complementary to the aforementioned works, the major contributions of this work are summarized below:

- We explore co-deployment of V-VLC and V-RF communication systems for relaying BSMs at road intersection. We consider data transmission using either V-VLC link or V-RF link at certain time instance. Parallel combination of V-VLC and V-RF links leads to improved outage performance, throughput, and reliability of the overall system. We compare the performance of proposed hybrid V-VLC/V-RF network with standalone V-VLC and standalone V-RF network using various analytical tools of stochastic geometry.
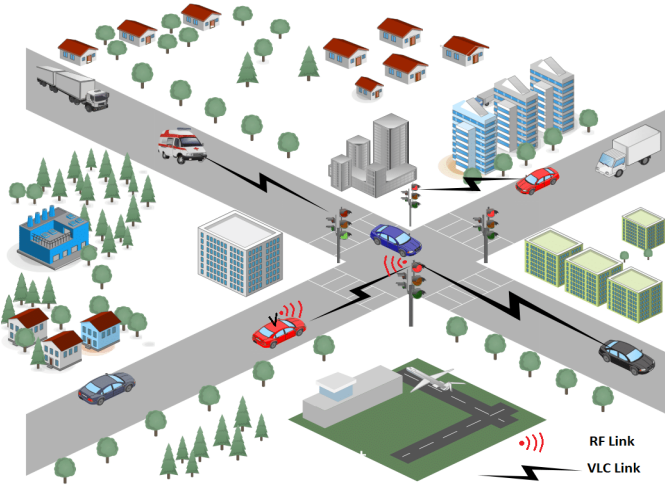
Fig. 1. Illustration of safety message dissemination in a vehicular network at road intersection. A desired vehicle can communicate with RSU via VLC shown by zig-zag or RF link shown by red transmission signal.

- We show the limitation of standalone V-VLC over V-RF when the distance between the desired vehicle and RSU is less than the critical distance, referred to as "*dead zone*" region, which exists due to restricted field-of-view (FOV) of receiver.
- We compare the performance of spatial ALOHA and CSMA/CA MAC protocol based standalone V-VLC, standalone V-RF and hybrid V-VLC/V-RF network configuration for relaying BSMs at road intersection.
- We propose to use DOR and IOR as performance metrics to investigate the impact of latency on various network configurations. In practice, a large latency is intolerable for many safety/warning related messages. These data oriented characterization can be applied to develop an upper bound on queuing performance over point-to-point vehicular communication links.

Numerical results illustrate that the implementation of MAC protocol based hybrid V-VLC/V-RF network leads to considerable improvement in outage performance, throughput and low latency as compared to stand-alone V-VLC or stand-alone V-RF network.

C. Paper Organization and Notations

1) Paper Organization: The organization of the paper is as follows: Section II describes the system model and assumption used for analysis. Section III presents detailed analytical framework to characterize the performance of standalone V-VLC, standalone V-RF and hybrid V-VLC/V-RF network configuration in terms of outage probability, throughput, DOR and IOR using various analytical tools of stochastic geometry. In Section IV, the simulation results and discussion are presented with useful insights. Finally, concluding remarks are given in Section V.

2) Notations: $\mathbb{P}[\cdot]$ denotes the probability of an event, $\mathbb{E}_Y[\cdot]$ is the expectation of its argument over random variable (RV) Y
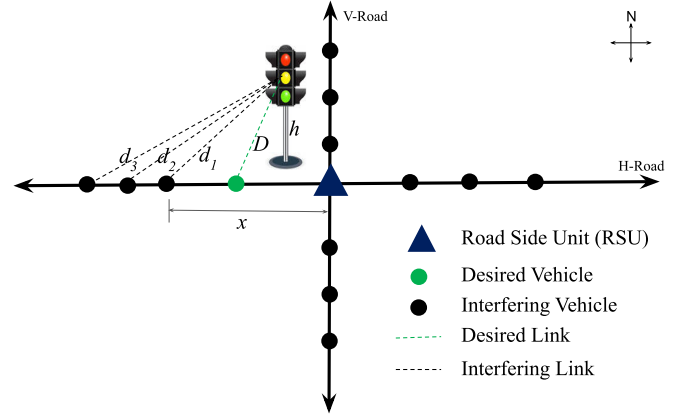

Fig. 2. Abstraction used for modelling. The desired vehicle is marked in green circle, while RSU is marked in triangle, is assumed to be located at the center of road intersection. All links can either be V-VLC or V-RF link.

and $\mathscr{L}$ denotes Laplace transform of a function. $\mathcal{F}_X(\cdot)$ denotes cumulative distribution function of an RV X.

II. PRELIMINARIES AND ASSUMPTION

A. Network Model

We consider an intersection scenario with two perpendicular roads, as shown in Fig. 1. For ease of analysis, it is assumed that each road carry a stream of interfering vehicles modeled as one-dimensional homogeneous PPPs. The intensities of interfering vehicles on H-road (located behind desired vehicle) and V-road are denoted by λ_H and λ_V respectively, and the PPPs describing the locations of the vehicles on the two roads are represented by $\phi_H \backsim \mathrm{PPP}\,(\lambda_H)$ and $\phi_V \backsim \mathrm{PPP}\,(\lambda_V)$ respectively. Each vehicle periodically generates a packet containing some information collected on board, such as the vehicle position, speed, acceleration and flow of direction. The desired vehicle close to intersection is assumed to carry critical road information which needs to be immediately communicated to RSU. Both VLC and IEEE 802.11p transceivers are assumed integrated on board and can be used separately (also called standalone V-VLC or V-RF network) or jointly (also called Hybrid V-VLC/V-RF network). The RSU is assumed to be positioned at the cross roads; RSUs for 802.11p are already installed, while RSUs for VLC can be considered integrated in the road lamps or traffic lights. When V-VLC is addressed, the communication between vehicle and RSU happen through head or rear LED headlamp, while the reception at RSU is carried out through photodetectors.

Fig. 2 portrays a generalized and simplified abstraction model of the proposed scenario. All links can either be VLC link (standalone V-VLC network) or RF link (standalone V-RF network). Both VLC as well as RF link are assumed to be available for hybrid V-VLC/V-RF network configuration. Vehicles on horizontal road H and vertical road V, represented by black circle, transmit concurrently and cause interference. Interestingly, unlike V-RF communication, based on practical receiver implementation, V-VLC suffers interference from vehicles on the same lane. As shown in Fig. 3, there also exists
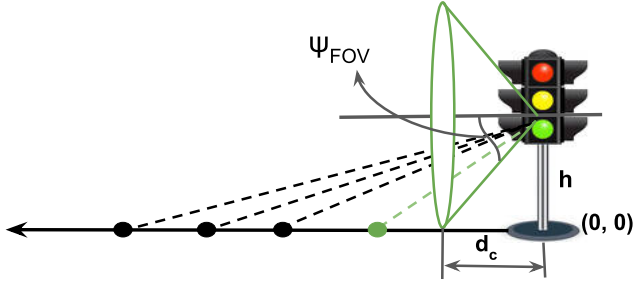
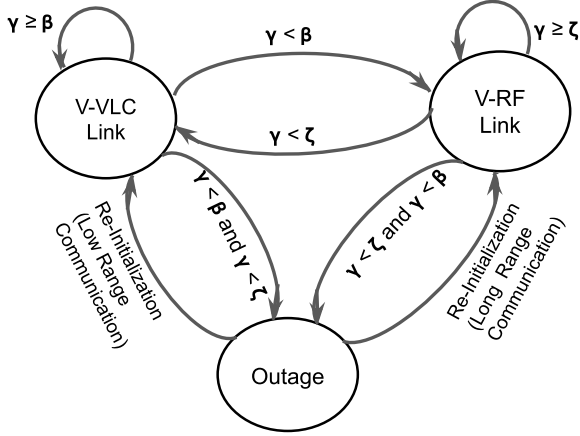Fig. 3. Illustration of critical distance, d_c. Here, $d_c = h/\tan(\psi_{FOV})$.

Fig. 4. Transition diagram of hybrid V-VLC/V-RF network configuration. Here, β and ζ denote the SINR threshold for standalone V-VLC and V-RF networks, respectively.

a critical distance, d_c, below which V-VLC may become un-operational (referred to as "dead zone" region for V-VLC). In such case, V-RF communication is the only feasible means of communication between the desired vehicle and RSU.

Fig. 4 shows transition diagram of hard switching based hybrid V-VLC/V-RF network configuration. An outage occurs when both V-VLC and V-RF links fall into outage. Re-initialization is decided depending upon the distance between the desired vehicle and RSU. In general, unlike V-RF, V-VLC network is a reliable option for low communication range.

B. Channel Model for V-VLC and V-RF

For a V-VLC system, the channel DC gain between k-th user and RSU can be modeled using Lambertian emission model as follows [34]

$$h_k = \frac{(m+1)A_R}{2\pi d_k^2} \cos^m(\phi_k) \cos(\Psi_k) T_s(\Psi_k) G(\Psi_k), \quad (1)$$

where, A_R, d_k, ϕ_k, and Ψ_k denote the area of PD, the Euclidean distance between the kth vehicle and RSU, the angle of irradiance and the angle of arrival (AoA) respectively. $T_s(\Psi_k)$ denotes the gain of the optical filter at the receiver; In above, m is the order of the Lambertian model which is

given by $m = -\frac{\ln(2)}{\ln\left(\cos\left(\phi_{\frac{1}{2}}\right)\right)}$. $G(\Psi_k)$ denotes the gain of optical concentrator at the receiver front-end which is given as

$$G(\Psi_k) = \begin{cases} \frac{n^2}{\sin^2 \Psi_{FOV}}; & \text{if } 0 \le \phi_k \le \Psi_{FOV}, \\ 0; & \text{if } \phi_k > \Psi_{FOV}, \end{cases} \quad (2)$$

where n denotes the refractive index of the optical concentrator. Based on simple geometrical illustration shown in Fig. 2, one can observe that $\cos(\phi_k) = \cos(\psi_k) = \frac{x_k}{\sqrt{(h^2+x_k^2)}}$ where, h denotes the height of RSU. (1) can be rewritten as:

$$h_k = \frac{(m+1)A_R}{2\pi} \frac{x_k^{(m+1)}}{(h^2 + x_k^2)^{\frac{(m+3)}{2}}} T_s(\Psi_k) G(\Psi_k), \quad (3)$$

The channel power can be obtained as: $Z_k^{V-VLC} = (h_k)^2$. In case of V-RF communication, we assume that the received signal amplitude in RF based V2V channel follows Rayleigh probability distribution function (PDF). Since Rayleigh fading is considered, fading gain (h_x) is an exponential random variable of unit mean.

C. MAC Protocols

In this section, we provide a brief introduction on MAC protocols such as slotted ALOHA, and CSMA/CA which have been well studied in literature [35]–[38]. The MAC protocol governs when a particular user can access the channel, and helps to reduce the overwhelming amount of interference from other users in a network. The two most common MAC protocols used for ad-hoc networks are slotted ALOHA and CSMA/CA. Besides, several MAC protocols have been proposed for VANET safety applications [35]–[37]. In slotted ALOHA, nodes that have a packet to send, access the channel during a time slot with a transmission probability $\rho \in [0, 1]$. In contrary, in CSMA, before sending a packet, a node verifies that whether the channel is free by listening to the channel. Only if the channel is free, the node transmits the packet. If the channel is busy, the node is forced to wait a random back-off time before it can try again [38]. In this work, we compare performance of spatial ALOHA and CSMA based MAC protocols which has not been investigated in context of V-VLC communication.

D. Intensity of Interfering PPP

The interference's intensity λ_{MAC} typically depends on the type of MAC that is being utilized. We compare the performance of the proposed scenario between two cases: slotted ALOHA with transmission probability, $\rho \in [0, 1]$ and CSMA/CA with contention region with radius, $\delta \ge 0$.

- **Slotted ALOHA**: For slotted ALOHA MAC, time axis is divided into slots and each transmitting vehicular node accesses the channel independently at each time-slot with a certain probability, $\rho \in [0, 1]$ on each road [39], [40]. This in turn leads to an independent thinning of the PPPs, so that $\lambda_{MAC} = \rho \lambda_R$. Here, λ_R denotes the intensity of interfering vehicles on each road.
- **CSMA**: For a CSMA MAC, a vehicle is allowed to transmit only if it has the lowest random timer within

its contention region (sensing range). This implies that (i) the intensity is a function of transmitter's location as other transmitting vehicles (interferers) in its contention region are forced to keep silent when the desired vehicle is active; (ii) the interference from the H- and V-roads is not independent. When the desired vehicle is active and transmitting at a distance, say $R(= \sqrt{D^2 - h^2})$, the resulting intensity of the PPPs used to approximate the PP of interferers can be expressed as [39]

$$\lambda_{MAC}^H = \begin{cases} p_A(x)\lambda_R & \text{if } x < -R-\delta, x > \delta - R \\ 0; & \text{otherwise,} \end{cases} \quad (4)$$

$$\lambda_{MAC}^V = \begin{cases} p_A(y)\lambda_R & \text{if } \|y\| > \sqrt{\delta^2 - R^2}, \\ 0; & \text{if } \|y\| \le \sqrt{\delta^2 - R^2}, \end{cases} \quad (5)$$

In (4) and (5), $p_A(x)$ and $p_A(y)$ denotes the access probability of interfering vehicle from H-road and V-road respectively. The access probability (which is used to thin the original process) is the probability that the given node has the smallest random timer in the corresponding contention region [39]. For CSMA MAC protocol, access probability is governed by [39, Eq.12]. In next section, we briefly describe various performance metrics such as outage probability, throughput, DOR and IOR for all slotted ALOHA based network configurations. Note that the closed form results using CSMA are hard to obtain, consequently it can be evaluated numerically as in [39].

III. PERFORMANCE METRICS

A. Outage Probability

In this subsection, we characterize the performance of the V-VLC in the presence of the aggregate interference and noise variance, σ^2 in terms of outage probability as a performance metric using moment generating functional (MGF) approach. In an interference limited channels, an outage occurs when the SINR falls below a given SINR threshold, β [23]. Mathematically,

$$\begin{aligned} P_{out,VLC}(\beta) &= \mathbb{P}(\mathcal{SINR} < \beta), \\ &= \mathbb{P}\left(\frac{\mathcal{S}}{\mathcal{I} + \sigma^2} < \beta\right). \end{aligned} \quad (6)$$

The desired electrical signal power $\mathcal{S}$ and interference $\mathcal{I}$ can be formulated as

$$\begin{aligned} \mathcal{S} &= \mathcal{R}^2 Z_o P_{VLC}, \\ \mathcal{I}_{V\mathcal{LC}} &= \sum_{x_k \in \phi_{PPP}} \mathcal{R}^2 Z_k P_{VLC}. \end{aligned} \quad (7)$$

In above, P_{VLC} and $\mathcal{R}$ denote the transmission power for V-VLC and the responsivity of PD respectively. The electrical SINR can be represented as:

$$\mathcal{SINR} = \frac{1}{\frac{\mathcal{I}}{\mathcal{R}^2 Z_o P_{VLC}} + \frac{1}{\alpha_0}}, \quad (8)$$

where $\alpha_0 = \frac{\mathcal{R}^2 Z_o P_{VLC}}{\sigma^2}$. From [8], the outage probability for V-VLC assuming that desired vehicle is transmitting can be given as:

$$P_{out,VLC}(\beta) = \mathbb{P}\left(\frac{\mathcal{I}}{\mathcal{R}^2 Z_o P_{VLC}} + \frac{1}{\alpha_0} > \frac{1}{\beta}\right). \quad (9)$$

We define random variable W as

$$W = \frac{\mathcal{I}}{\mathcal{R}^2 Z_o P_{VLC}} + \frac{1}{\alpha_0}, \quad (10)$$

Hence, Eq. (9) can be rewritten as

$$P_{out,VLC}(\beta) = \mathbb{P}(W > \beta^{-1}) = 1 - \mathcal{F}_W(\beta^{-1}). \quad (11)$$

In general, it is quite difficult to obtain a closed-form solution for $\mathcal{F}_W(\beta^{-1})$. Hence, we make use of numerical inversion of Laplace transform to find CDF, $\mathcal{F}_W(\beta^{-1})$. The CDF of a random variable W is related to the Laplace transform of $\mathcal{F}_W(w)$ as

$$\mathcal{F}_W(w) = \frac{1}{2\pi j} \int_{c-j\infty}^{c+j\infty} \mathcal{L}_{\mathcal{F}_W(w)} \exp(sw) ds. \quad (12)$$

where j denotes imaginary unit ($\sqrt{-1}$). The above integral can be discretized to get a series using the trapezoid rule and then the infinite series can be truncated to get a finite sum using the Euler summation [41]. Also, $\mathcal{L}_{\mathcal{F}_W(w)}(s) = \frac{\mathcal{L}_W(s)}{s}$. Moreover, (11) can be approximated as

$$P_{out,VLC}(\beta) \approx 1 - \frac{2^{-B} \exp(\frac{A}{2})}{\beta^{-1}} \sum_{b=0}^{B} \binom{B}{b} \sum_{c=0}^{C+b} \frac{(-1)^c}{D_c} Re\left\{\frac{\mathcal{L}_W(s)}{s}\right\}. \quad (13)$$

where $D_c = 2$ (if $c = 0$) and $D_c = 1$ (if $c = 1, 2, 3,..$) and $s = \frac{(A+j2\pi c)}{2\beta^{-1}}$. The estimation error is controlled by three parameters A, B and C. Using the well established result given in [41] and [42], in order to achieve an estimation accuracy of $10^{-\eta}$ (i.e., having the $(\eta-1)$th decimal correct), A, B and C have to be at least equal to $\eta \ln 10$, 1.243η-1, and 1.467η, respectively. Setting $A = 8\ln 10$, $B = 11$, $C = 14$ achieves stable numerical inversion with an estimation error of 10^{-8}.

Using the definition of the Laplace transform of the probability distribution of a random variable,

$$\begin{aligned} \mathcal{L}_W(s) &= \mathbb{E}_{\mathcal{I}}\left[\exp\left(-s\left(\frac{\mathcal{I}}{\mathcal{R}^2 Z_o P_{VLC}} + \frac{1}{\alpha_0}\right)\right)\right], \\ &= \mathbb{E}_{\mathcal{I}}\left[\exp\left(-\frac{s}{\alpha_0}\right) \exp\left(-\frac{s\mathcal{I}}{\mathcal{R}^2 Z_o P_{VLC}}\right)\right], \\ &= \exp\left(-\frac{s}{\alpha_0}\right) \\ &\quad \times \mathbb{E}_{\phi_{PPP}}\left[\prod_{x \in \phi_{PPP}} \exp\left(-\frac{sk'x^{2(m+1)}}{Z_o(h^2+x^2)^{(m+3)}}\right)\right]. \end{aligned} \quad (14)$$

Here $k' := \left(\frac{(m+1)A_R}{2\pi} T_s(\psi)G(\psi)\right)^2$. The expectation in (14) can be solved using probability generating functional Laplace (PGFL)[1] defined for a homogeneous Poisson point

---

[1]The PGFL can be envisioned as an equivalent for point process of the characteristic function (CF) or moment generating function (that provide an alternative description of random variables). It enables to compute the Laplace transform (LT) of random variables of the form $F = \sum_{X_i \in \Psi_{PPP}} g(X_i)$. In mathematical form, LT of such function can be given as:

$$\mathcal{L}(s) = \mathbb{E}[e^{-sF}] = \mathbb{E}\left[\exp(-s \sum_{X_i \in \Psi} g(X_i))\right] = \mathbb{E}\left[\prod_{X_i \in \Psi} e^{-sg(X_i)}\right]$$

6

process [23, Th 4.9].

$$\mathbb{E}_{\phi_{PPP}}\left[\prod_{x\epsilon\phi_{PPP}}\exp\left(-\frac{sk'x^{2(m+1)}}{Z_o(h^2+x^2)^{(m+3)}}\right)\right]=$$

$$\exp\left[-\lambda_{MAC}\int_{-\infty}^{-R}\left(1-\exp\left(-\frac{sk'x^{2(m+1)}}{Z_o(h^2+x^2)^{(m+3)}}\right)\right)dx\right].$$
$$0\le\phi_k\le\Psi_{\text{FOV}}$$
(15)

The Eq. (15) can be determined numerically using standard software tools like MATLAB or MATHEMATICA.

Assuming free space path loss propagation model, the interference experienced at RSU for RF based V2V communication can be expressed as sum of RF power received from all the interferers as

$$I_{RF}=\sum_{x\epsilon\Phi_{PPP}}P_{RF}G_tG_r\ell h_x(h^2+x^2)^{-\frac{\alpha}{2}},\qquad(16)$$

where $\ell=\frac{c^2}{(4\pi)^2f_0^2}$. In above expression, P_{RF}, α, G_t and G_r are the transmission power for V-RF, the path loss exponent, the antenna gains for transmitter and receiver respectively [43]. In order to calculate outage probability $P_{out,RF}(\zeta)$, it is more convenient to express it as a function of probability of successful transmission, $P_s(\zeta)$, where $P_{out,RF}(\zeta)$ can be expressed as

$$P_{out,RF}(\zeta)=1-P_s(\zeta)\qquad(17)$$

The probability of successful transmission, $P_s(\zeta)$ can be calculated as

$$P_s(\zeta)=\mathbb{P}(\mathcal{SINR}>\zeta),$$
$$=\mathbb{P}\left(\frac{P_{RF}G_tG_r\ell h_xD^{-\alpha}}{I_H+I_V+\mathcal{N}_0}>\zeta\right),$$
$$=\mathbb{E}_{I_H+I_V}\left[\mathbb{P}\left(h_x>\frac{\zeta}{P_{RF}G_tG_r\ell D^{-\alpha}}(I_H+I_V+\mathcal{N}_0)\right)\right],$$
$$=\exp\left(-\frac{\zeta\mathcal{N}_0}{P_{RF}G_tG_r\ell D^{-\alpha}}\right)$$
$$\times\mathbb{E}_{I_H+I_V}\left[\exp\left(-\frac{\zeta(I_H+I_V)}{P_{RF}G_tG_r\ell D^{-\alpha}}\right)\right],$$
$$=\underbrace{\mathscr{L}_{I_H}\left(\frac{\zeta}{P_{RF}G_tG_r\ell D^{-\alpha}}\right)}_{1^{st}}\underbrace{\mathscr{L}_{I_V}\left(\frac{\zeta}{P_{RF}G_tG_r\ell D^{-\alpha}}\right)}_{2^{nd}}$$
$$\times\underbrace{\exp\left(-\frac{\zeta\sigma^2}{P_{RF}G_tG_r\ell D^{-\alpha}}\right)}_{3^{rd}}.$$
(18)

where $\mathscr{L}(.)$, I_H and I_V denote the Laplace transform, the interference from H-road and V-road respectively. Kindly note that there are three factors in (18) which can be interpreted as follows: the first and second factor represent the reduction in probability of successful transmission taking into consideration the impact of interference from the interferers from H-road and V-road respectively; the third factor denotes the probability of successful transmission for interference-free scenario. For a one-dimensional PPP, the Laplace transform

of the aggregate interference originating from the interferers can be given as

$$\mathscr{L}_{I_V}(s)=\mathbb{E}[\exp(-sI_{RF})],$$
$$=\mathbb{E}\left[\prod_{x\epsilon\phi}\exp(-sP_{RF}G_tG_r\ell h_x(h^2+x^2)^{-\frac{\alpha}{2}})\right],$$
$$\overset{(a)}{=}\mathbb{E}_x\left[\prod_{x\epsilon\phi}\mathbb{E}_{h_x}\{\exp(-sP_{RF}G_tG_r\ell h_x(h^2+x^2)^{-\frac{\alpha}{2}})\}\right],$$
$$=\mathbb{E}_x\left[\prod_{x\epsilon\phi}\frac{1}{1+sP_{RF}G_tG_r\ell(h^2+x^2)^{\frac{-\alpha}{2}}}\right],$$
$$\overset{(b)}{=}\exp\left(-2\lambda_{MAC}\int_0^\infty\frac{1}{1+(h^2+x^2)^{\frac{\alpha}{2}}/sP_{RF}G_tG_r\ell}dx\right),$$
(19)

Here (a) holds due to independence of fading coefficients h_x, (b) uses the definition of PGFL for PPP.
Special Case: The step (b) can be further expressed in simplified form by setting the path loss exponent, $\alpha=2$ as

$$\mathbb{E}[\exp(-sI_{RF})]=\exp\left(-\lambda_{MAC}\frac{\pi(sP_{RF}G_tG_r\ell)}{\sqrt{h^2+sP_{RF}G_tG_r\ell}}\right),\quad(20)$$

Substituting $s=\frac{\zeta}{P_{RF}G_tG_r\ell D^{-\alpha}}$ yields the result as

$$\mathscr{L}_{I_V}\left(\frac{\zeta}{P_{RF}G_tG_r\ell D^{-\alpha}}\right)=\exp\left(-\lambda_{MAC}\frac{\pi\zeta D^\alpha}{\sqrt{h^2+\zeta D^\alpha}}\right).\quad(21)$$

Corollary: When the height of RSU is very low, the step (b) can also be expressed in alternative form as:

$$\mathbb{E}[\exp(-sI_{RF})]=\exp\left(-2\lambda_{MAC}(sP_{RF}G_tG_r\ell)^{\frac{1}{\alpha}}\frac{\pi}{\alpha}\csc(\frac{\pi}{\alpha})\right),$$
(22)

Substituting $s=\frac{\zeta}{P_{RF}G_tG_r\ell D^{-\alpha}}$ yields the result as

$$\mathscr{L}_{I_V}\left(\frac{\zeta}{P_{RF}G_tG_r\ell D^{-\alpha}}\right)=\exp\left(-2\lambda_{MAC}(\zeta)^{\frac{1}{\alpha}}D\frac{\pi}{\alpha}\csc\left(\frac{\pi}{\alpha}\right)\right).$$
(23)

$$\mathscr{L}_{I_H}\left(s=\frac{\zeta}{P_{RF}G_tG_r\ell D^{-\alpha}}\right)=$$
$$\exp\left(-\lambda_{MAC}\left[\int_{-\infty}^{-R}\frac{1}{1+(h^2+x^2)^{\frac{\alpha}{2}}/s\zeta D^\alpha}dx+\right.\right.$$
$$\left.\left.\int_0^\infty\frac{1}{1+(h^2+x^2)^{\frac{\alpha}{2}}/s\zeta D^\alpha}dx\right]\right).$$
(24)

We now drive the expression for outage probability of a hard-switching based hybrid V-VLC/V-RF network. Hard switching based hybrid V-VLC/V-RF network considers only single link to be operational. For simple receiver implementation, it is assumed that only one of the links is active at a certain point. The outage probability of such hybrid network configuration can given as[2]

$$P_{out,hyb}(\beta,\zeta)\ge P_{out,VLC}(\beta)P_{out,RF}(\zeta).\qquad(25)$$

[2]Note that the equality holds when V-VLC and V-RF links are considered to be independent.

B. Throughput

From a system design perspective, the outage probability can not be considered as sufficient metric to characterize the performance, since a MAC that allows few concurrent transmissions leads to high packet reception probabilities but low throughput as well. Hence, to suitably compare the impact of different MAC protocols, it is necessary to characterize the throughput for the intersection scenario for different network configuration. For the case with desired transmitter located at x_{tx}, the throughput for a specific network configuration with system bandwidth, B_s and SINR threshold, β can be expressed as [39]

$$\mathcal{T} = p_A(x_{tx})(1 - P_{out})\log_2(1 + \beta)B_s. \qquad (26)$$

where $p_A(x_{tx})$ denotes the access probability of a transmitter located at x_{tx} [39].

C. Data Oriented Characterization: DOR and IOR

Many safety/warning related messages are so critical that a large latency is intolerable especially during accident prone scenarios. DOR and IOR can be of strong interest to vehicular communication and can be used to compare the performances of standalone V-VLC and V-RF based on offering high reliability as well as low latency. Any vehicular transmission systems should be able to efficiently support the large amount of data traffics with tolerable latency. As such, we make use of a data-oriented metric, minimum transmission time (MTT) which is defined as the minimum time duration required to transmit a certain amount of data, H over a channel with bandwidth, B. Then, the DOR can be defined as the probability that MTT required for transmitting a certain amount of data is greater than a predefined delay threshold duration [44]. Mathematically,

$$DOR^{MAC} = \mathbb{P}(MTT > T_{th}), \qquad (27)$$

where T_{th} denotes the delay threshold duration and can be related to the delay requirement of the data to be transmitted. As a matter of fact, DOR may serve as an statistical measure for the quality of service experienced by individual data transmission for stringent delay requirement by a particular network. Irrespective of multiple access scheme, the DOR for small data transmission within a given coherence time can be defined as

$$DOR^{MAC} = \mathbb{P}\left(SINR < 2^{\frac{H}{BT_{th}}} - 1\right). \qquad (28)$$

Apart from DOR analysis, the characterization of the amount of data that can be successfully transmitted over a specific spectral-temporal resource block also needs to be taken into account for any vehicular transmission system. We make use of another data oriented metric, maximum entropy throughput (MET) which is defined as the maximum amount of information that can be transmitted over a certain time duration, T and system channel bandwidth B. Then, the IOR can be defined as the probability that MET over a certain time duration is less than a threshold entropy value, represented by H_{th} [44]. Mathematically,

$$IOR^{MAC} = \mathbb{P}\left(SINR < 2^{\frac{H_{th}}{BT}} - 1\right). \qquad (29)$$

TABLE I
V-VLC and V-RF system parameters

| Parameter	Symbol	Value
Lambertian Order	m	1
PD active detection area	A_d	$1 \ cm^2$
Half angle of PD's field of view (FOV)	Ψ_{FOV}	$60°$
LED semi-angle	$\Phi_{\frac{1}{2}}$	$70°$
Transmission power for V-VLC	P_{VLC}	36.5 dBm [45]
Transmission power for V-RF	P_{RF}	23 dBm [46]
Noise PSD in VLC	σ^2	10^{-22} W/Hz
Noise PSD in RF	$\mathcal{N}_0$	-174 dBm/Hz
RF path loss exponent	α	4
Absolute temperature	T_k	$298°$ K
System Bandwidth	B_s	20 MHz
Optical filter gain	$T_s(\Psi_k)$	1
Refractive index	n	1.5
Height of LED traffic light	h	8 m
Access Probability	ρ	0.01-0.9
Traffic Intensity	λ_R	0.01
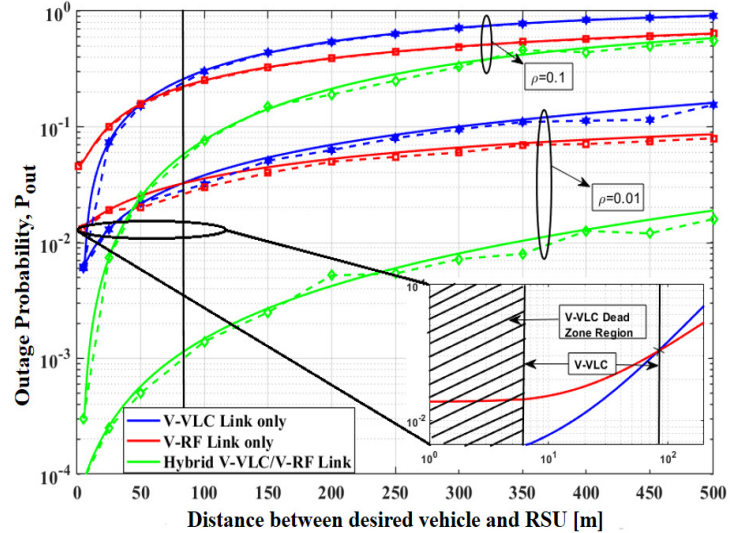
Fig. 5. Comparison of analytical (solid line) and simulation (dashed line) results for outage probability, P_{out} versus distance for V-VLC links only (blue), V-RF links only (red) and hybrid V-VLC/V-RF Links (green) with slotted ALOHA protocol.

IV. NUMERICAL RESULTS AND DISCUSSION

In this section, we present numerical results that substantiate our theoretical findings. The system model parameters are adopted in accordance with practical vehicular scenario and listed in Table I. Specifically, we show the potential benefit of standalone V-VLC/V-RF links or hybrid V-VLC/V-RF links. In order to validate the accuracy of our theoretical findings, Monte Carlo simulations are performed by averaging over 10,000 realizations of PPPs and fading channel parameters. We consider a worst case scenario where interference from interferers arise from infinite road segment ($\mathcal{B} = \mathbb{R}^1$).

Fig. 5 gives comparison of outage performance for standalone V-VLC links, V-RF links and hybrid V-VLC/V-RF links with slotted ALOHA protocol. We observe that when
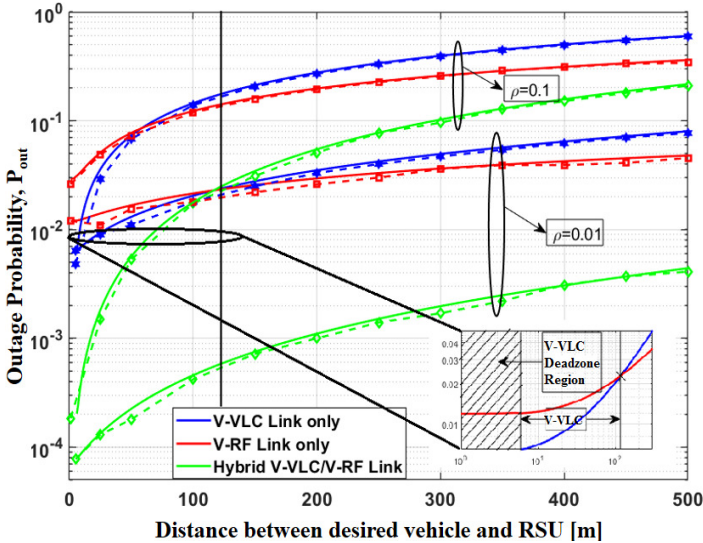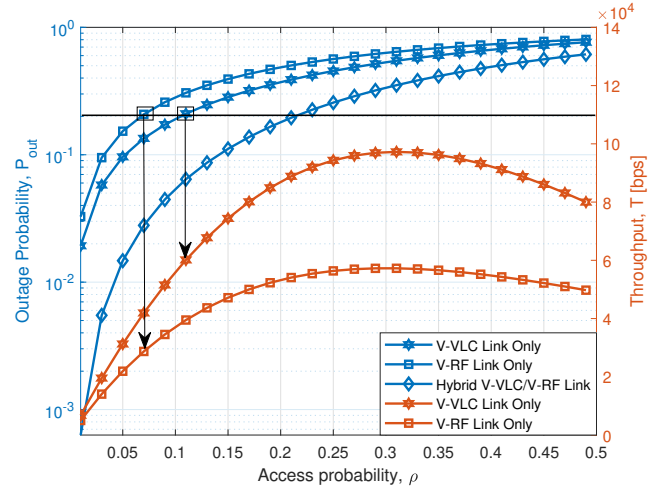
Fig. 6. Comparison of analytical (solid line) and simulation (dashed line) results for outage probability, P_{out} versus distance for V-VLC link only (blue), V-RF link only (red) and hybrid V-VLC/V-RF link (green) with CSMA CA protocol.

(a) Outage probability, P_{out} and throughput, $\mathcal{T}$ as a function of access probability, ρ for standalone V-VLC links, V-RF links and hybrid V-VLC/V-RF links when distance between the desired vehicle and RSU, R is 50 m.

(b) Outage probability, P_{out} and throughput, $\mathcal{T}$ as a function of access probability, ρ for standalone V-VLC links, V-RF links and hybrid V-VLC/V-RF links when distance between the desired vehicle and RSU, R is 150 m.
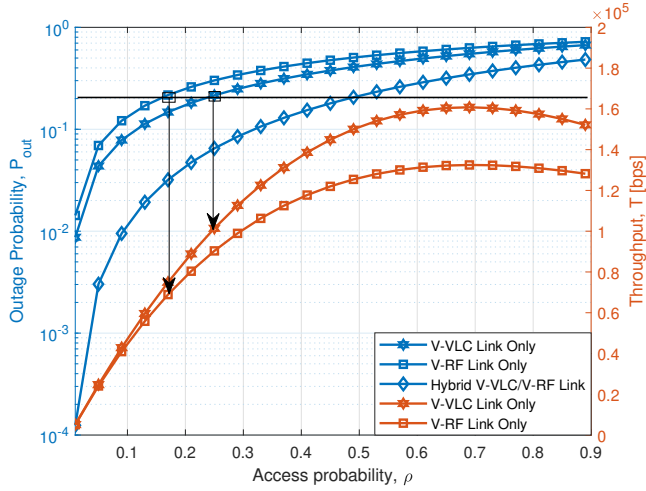
Fig. 7. Outage Probability, P_{out} and Throughput, $\mathcal{T}$ as a function of access probability, ρ for slotted ALOHA case.

desired transmitter's location from RSU increases, the outage probability increases. Also, the outage performance of standalone V-VLC links is comparatively better than standalone V-RF for low communication range. For instance, when access probability, ρ=0.01, the outage performance of standalone V-VLC links is better compared to V-RF links when desired transmitter's location is upto 80 m. However, standalone V-RF is reliable option for long distance communication. It can also be noted that there exits limitation of standalone V-VLC over V-RF when distance between the desired vehicle and RSU is less than 5 m which comes at the cost of restricted receiver's FOV. We consider the lower bound of Eq. 25 for plotting simulation results for outage probability associated with hybrid V-VLC/V-RF network configuration. It is worth mentioning here that irrespective of distance between the desired vehicle and RSU, a hybrid V-VLC/V-RF links outperforms standalone V-VLC or V-RF link as expected. Let us recall that hybrid outage is a joint event of V-VLC and V-RF links wherein the outage probability of hybrid V-VLC/V-RF will be less than the outage probability associated with either standalone V-VLC or V-RF links. However, this comes at the expense of extra resources required during practical implementation of a hybrid V-VLC/V-RF links.

We further study the performance gain achieved in proposed scenario by using CSMA over slotted ALOHA. We set CSMA contention radius, δ=10 m. Fig. 6 illustrates that for access probability, ρ=0.01, the outage performance of standalone V-VLC links is better compared to V-RF links when desired transmitter's location, $R < 120$ m. However, standalone V-RF is reliable option when desired transmitter's location, $R > 120$ m. As before, hybrid V-VLC/V-RF links outperforms standalone V-VLC and V-RF links. Interestingly, a low access probability reduces the outage probability. For ease of validation and visualization, we plot outage probability, P_{out} as a function of access probability, ρ as can be seen in Fig. 7 and
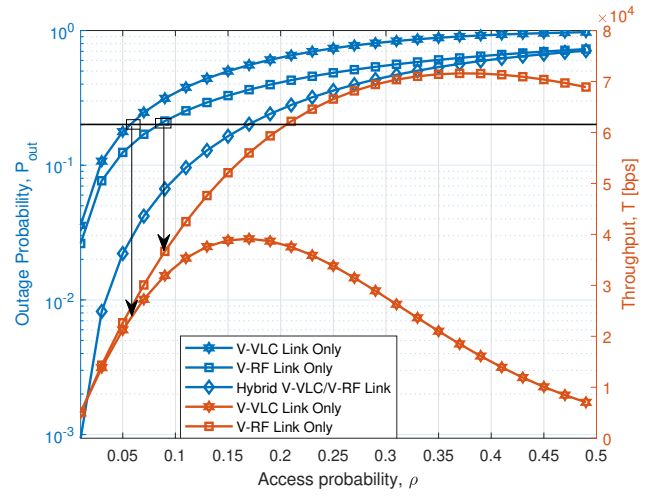
8.

We observe from Fig. 7 that for ALOHA case, with an increase in access probability, ρ outage probability increases due to the availability of more interferers. Also, the throughput first increases (due to more active transmitters) with increase in access probability and then decreases (due to extensive amount of interference), leading to an optimal value of access probability, ρ. Nevertheless, in order to ensure a certain quality of service, one must also consider a guarantee on the outage performance as well. With an outage probability below 20% when distance between the desired vehicle and RSU, $R = 50$ m, the optimal value of access probability for standalone V-VLC link, ρ=0.12, results in a throughput of about 60 Kbps as can be seen in Fig. 7a. In addition, the outage performance of standalone V-VLC is better than standalone V-RF. However, increasing the distance, R, the opposite trend can be observed

(a) Outage probability, P_{out} and throughput, T as a function of access probability, ρ for standalone V-VLC links, V-RF links and hybrid V-VLC/V-RF links when distance between the desired vehicle and RSU, R is 50 m.
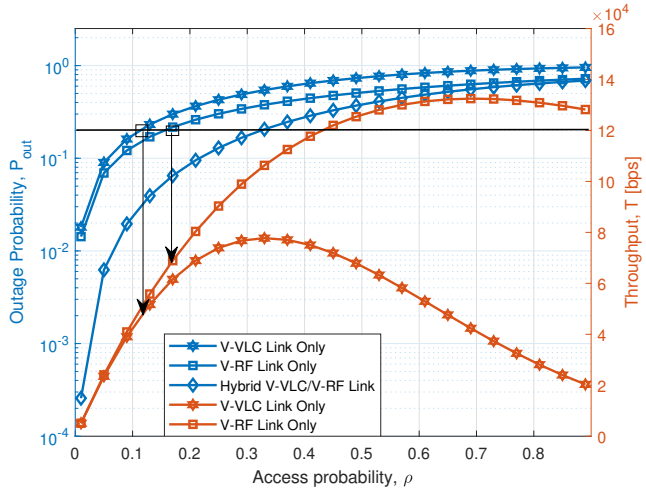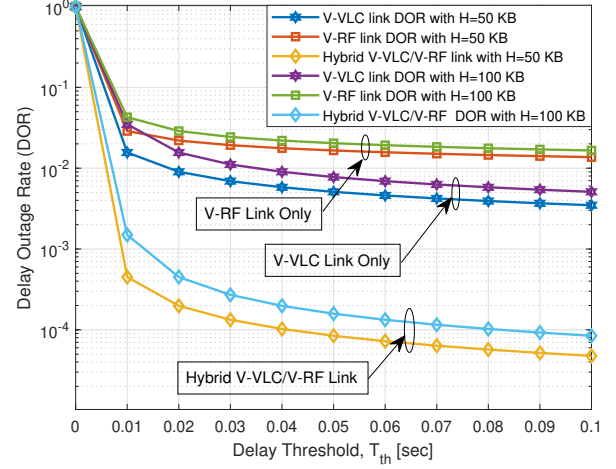

(a) DOR comparison for standalone V-VLC links, V-RF links and hybrid V-VLC/V-RF links when distance between the desired vehicle and RSU, R is 50 m and access probability, ρ is 0.01

(b) Outage probability, P_{out} and throughput, $\mathcal{T}$ as a function of access probability, ρ for standalone V-VLC links, V-RF links and hybrid V-VLC/V-RF links when distance between the desired vehicle and RSU, R is 150 m.
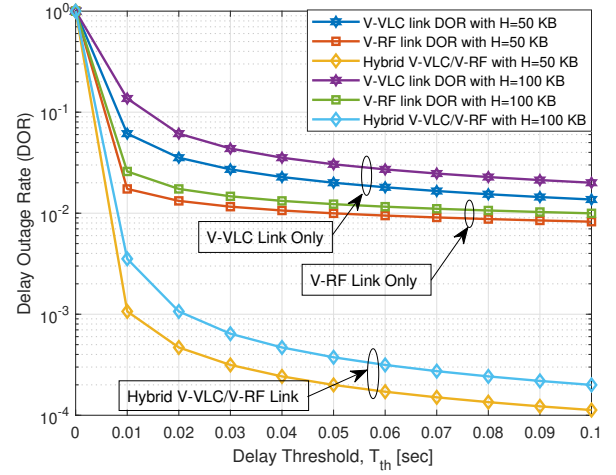
Fig. 8. Outage Probability, P_{out} and Throughput, $\mathcal{T}$ as a function of access probability, ρ for CSMA CA case.

(b) DOR comparison for standalone V-VLC links, V-RF links and hybrid V-VLC/V-RF links when distance between the desired vehicle and RSU, R is 150 m and access probability, ρ is 0.01

Fig. 9. Delay outage performance of V-VLC links only, V-RF links only and hybrid V-VLC/V-RF links for ALOHA case for two different distance between the desired vehicle and RSU.

in Fig. 7b. As expected, hybrid V-VLC/V-RF outperforms standalone V-VLC or V-RF in terms of outage performance. Kindly note that the throughput of hybrid V-VLC/V-RF system depends on maximum throughput offered by either standalone V-VLC or standalone V-RF system.

For CSMA (Fig. 8), large contention region (i.e., low access probability) reduces the outage probability. Analogous to ALOHA, the throughput first increases with increase in access probability, ρ and then decreases. To ensure an outage probability below 20% when distance between the desired vehicle and RSU, R = 50 m, the optimal value of access probability for standalone V-VLC links, ρ=0.25, results in a throughput of about 100 Kbps. Hence, in this scenario, the use of CSMA instead of ALOHA leads to more increase in the throughput for the same transmitter location. It can be inferred from above comparison that implementation of

hybrid V-VLC/V-RF links leads to considerable improvement in throughput and outage probability improvement, compared to scenarios utilizing either V-VLC links or V-RF links separately.

Fig. 9 compares DOR performance comparison for standalone V-VLC links, V-RF links and hybrid V-VLC/V-RF links with slotted ALOHA protocol. In particular, we plot DOR of both strategies as function of the delay threshold, T_{th} for different data amount $H \in \{50$ KB, 100 KB$\}$. We can observe that for both the choices of H, there exists complementary behaviour in DOR performance of standalone V-VLC and V-RF network depending on distance between the desired vehicle and RSU, R. Specifically, with access probability, ρ = 0.01 and transmitter's location, R=50 m, DOR performance of standalone V-VLC is comparatively better than V-RF as can be seen from Fig. 9a. The opposite is true when R is 150 m
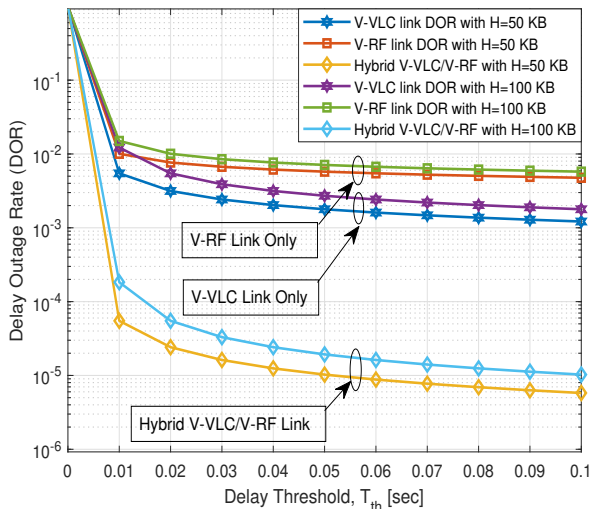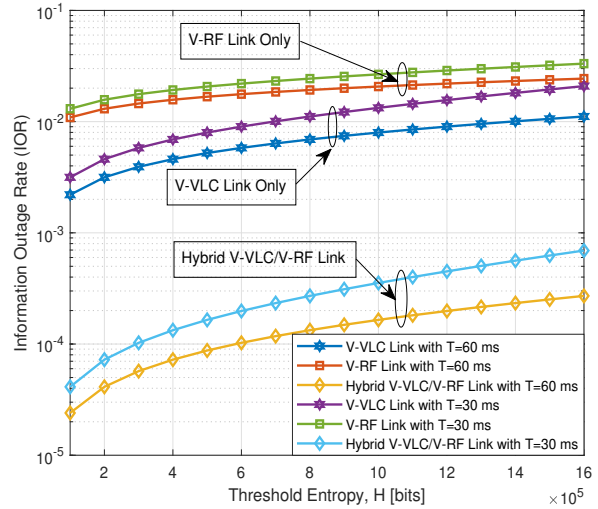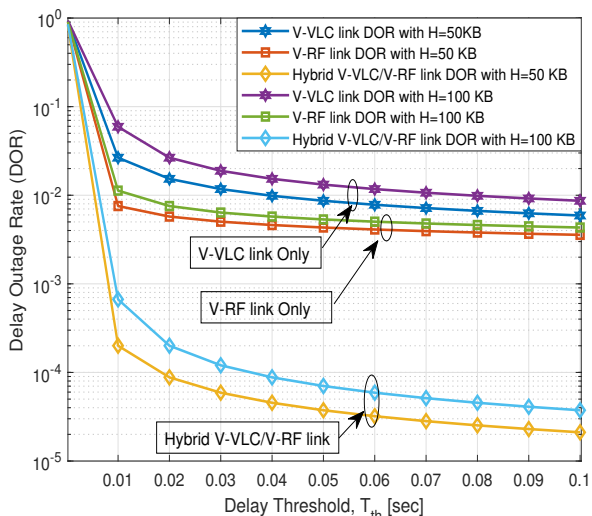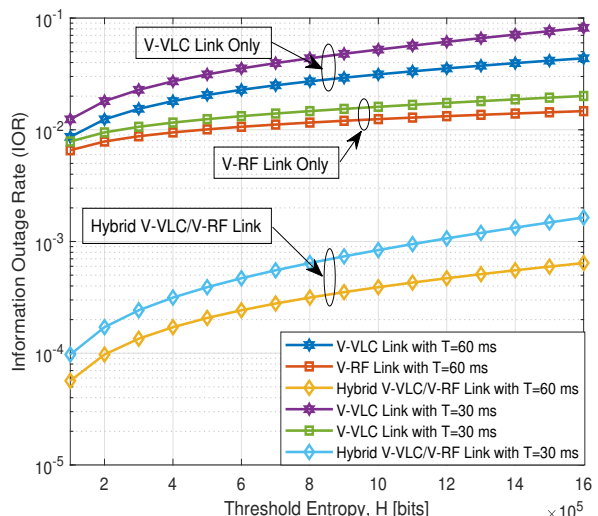
(a) R = 50 m

(b) R = 150 m

Fig. 10. Delay outage performance of V-VLC links only, V-RF links only and hybrid V-VLC/V-RF links for CSMA case for two different distance between the desired vehicle and RSU. Here, access probability, ρ is 0.01.

(a) R = 50 m

(b) R = 150 m

Fig. 11. Information Outage Rate of V-VLC links only, V-RF links only and hybrid V-VLC/V-RF links for slotted ALOHA case for two different distance between the desired vehicle and RSU. Here, access probability, ρ is 0.01.

as shown in Fig. 9b. As before, we observe DOR performance improvement by employing CSMA for both standalone V-VLC as well as V-RF network as depicted in Fig.10. The reason is as follows: DOR typically depends on SINR which is better for proposed scenario with CSMA/CA (due to low interference). It is interesting to note that for data traffic with stringent delay requirement, hybrid V-VLC/V-RF ensures minimum delay in transmitting given amount of information between the desired vehicle and RSU as compared to standalone V-VLC or V-RF network.

We now compare the IOR performance of standalone V-VLC, V-RF and hybrid V-VLC/V-RF network configuration for two different values on transmitter's location, $R \in \{50$ m, 150 m$\}$. In Fig. 11 and 12, we plot IOR for all network configuration with ALOHA and CSMA as a function of threshold entropy, H_{th} for two different time duration, $T \in \{60$

ms, 30 ms$\}$. In particular, Fig. 11a shows that for a given IOR performance with slotted ALOHA, standalone V-VLC links is reliable option over standalone V-RF links when distance between the desired vehicle and RSU, R is 50 m. However, the complementary insights stands true when D is 150 m as evident from Fig 11b.

In Fig. 12, we again observe the improvement in IOR performance of all the network configuration by using CSMA over ALOHA. The reason is as follows: IOR typically depends on SINR which is better for proposed scenario with CSMA/CA (due to low interference). Again, the performance of standalone V-VLC or V-RF link depends on distance between legitimate vehicle and RSU, R as evident from Figs 12a and 12b. It is worth mentioning that irrespective of distance, R, hybrid V-VLC/V-RF system always guarantees maximum amount of information flow between the desired vehicle and
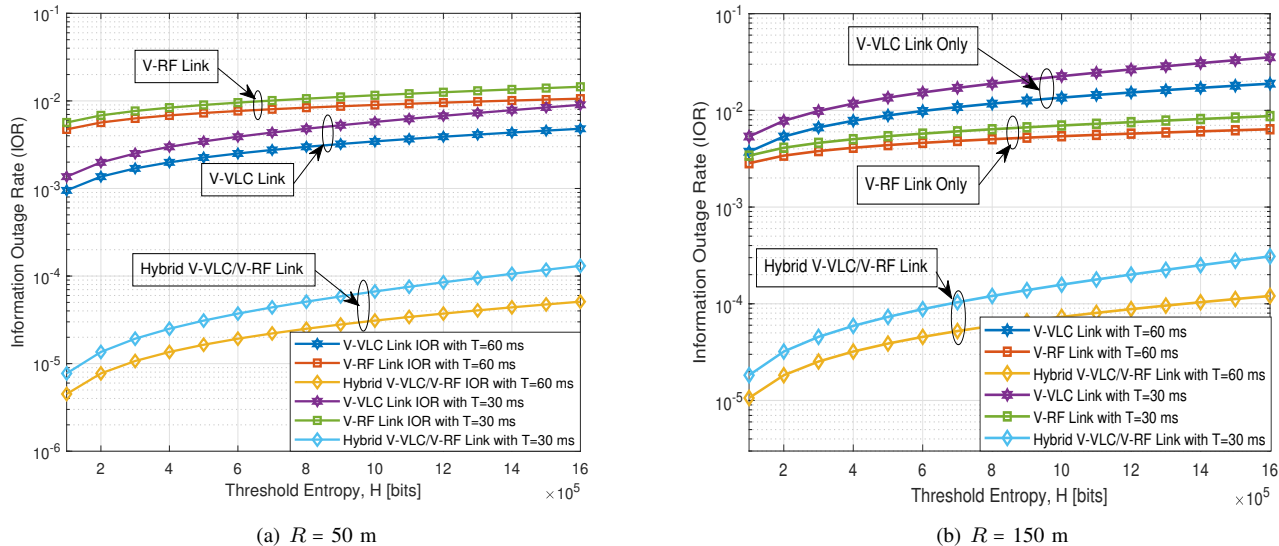
(a) $R = 50$ m

(b) $R = 150$ m

Fig. 12. Information Outage Rate of V-VLC links only, V-RF links only and hybrid V-VLC/V-RF links for CSMA case for two different distances between the desired vehicle and RSU. Here, access probability, ρ is 0.01.

Distance, R	Performance Metric	Standalone V-RF	Standalone V-VLC	Hybrid V-VLC/V-RF
R<120 m (Short Range Communication)	Outage Probability	★	★ ★	★ ★ ★
	Throughput	★	★ ★	★ ★
	Delay Outage Rate (DOR)	★	★ ★	★ ★ ★
	Information Outage Rate (IOR)	★	★ ★	★ ★ ★
120 m<R< 500 m (Long Range Communication)	Outage Probability	★ ★	★	★ ★ ★
	Throughput	★ ★	★	★ ★
	Delay Outage Rate (DOR)	★ ★	★	★ ★ ★
	Information Outage Rate (IOR)	★ ★	★	★ ★ ★

Rating criterion: ★: Poor, ★ ★: Average ★ ★ ★: Good

Note that the same trend can be observed for slotted ALOHA based MAC protocol as well.

TABLE II

Performance of various network configurations with CSMA based MAC protocol. Here, access probability ρ is assumed to be 0.01.

RSU as compared to standalone V-VLC or V-RF network in the given time duration.

The overall results can be best summarized in a tabular form. Table II summarizes performance of various network configurations with CSMA/CA based MAC protocol. The same trend can be observed for slotted ALOHA based MAC protocol as well.

V. CONCLUDING REMARKS

In this paper, we have shown the potential benefit of employing hybrid V-VLC/V-RF over standalone V-VLC or V-RF network configuration for BSMs dissemination at road intersection ensuring high reliability and low latency. Depending on transmitter's location, it is found that the standalone V-VLC and V-RF exhibit complementary roles in terms of outage probability, throughput, DOR and IOR. The presented framework also show the limitation of standalone V-VLC over V-RF communication when the distance between desired vehicle and RSU is less than the critical distance defined for

V-VLC system. We have also found that hybrid V-VLC/V-RF outperforms standalone V-VLC or V-RF network, thus serving as a better alternative option to meet diverse application needs for future intelligent transportation system. It is expected that this comparative analysis may stimulate more innovations for hybrid VLC/RF based vehicular networks.

ACKNOWLEDGMENT

REFERENCES

[1] H. Peng, Le Liang, X. Shen, and G. Y. Li, "Vehicular communications: A network layer perspective," *IEEE Trans. Veh. Technol.*, vol. 68, no. 2, pp. 1064–1078, 2019.

[2] M. Noor-A-Rahim, G. G. M. N. Ali, H. Nguyen, and Y. L. Guan, "Performance analysis of IEEE 802.11p safety message broadcast with and without relaying at road intersection," *IEEE Access*, vol. 6, pp. 23 786–23 799, Apr. 2018.

[3] C. F. Mecklenbrauker, A. F. Molisch, J. Karedal, F. Tufvesson, A. Paier, L. Bernadó, T. Zemen, O. Klemp, and N. Czink, "Vehicular channel characterization and its implications for wireless system design and performance," *Proc. IEEE*, vol. 99, no. 7, pp. 1189–1212, 2011.

[4] J. Santa, R. Toledo-Moreo, M. A. Zamora-Izquierdo, B. Úbeda, and A. F. Gómez-Skarmeta, "An analysis of communication and navigation issues in collision avoidance support systems," *Transportation Research Part C: Emerging Technologies*, vol. 18, no. 3, pp. 351–366, 2010.

[5] P. Ji, H.-M. Tsai, C. Wang, and F. Liu, "Vehicular visible light communications with LED taillight and rolling shutter camera," in *Proc. IEEE 79th Veh. Technol. Conf. (VTC Spring)*. IEEE, May. 2014, pp. 1–6.

[6] M. Noor-A-Rahim, Z. Liu, H. Lee, M. O. Khyam, J. He, D. Pesch, K. Moessner, W. Saad, and H. V. Poor, "6G for vehicle-to-everything (V2X) communications: Enabling technologies, challenges, and opportunities," *arXiv:2012.07753*, 2020.

[7] A. Bazzi, B. M. Masini, A. Zanella, and I. Thibault, "On the performance of ieee 802.11p and LTE-V2V for the cooperative awareness of connected vehicles," *IEEE Trans. Veh. Technol.*, vol. 66, no. 11, pp. 10 419–10 432, 2017.

[8] Y. Hu, H. Li, Z. Chang, and Z. Han, "End-to-end backlog and delay bound analysis for multi-hop vehicular ad hoc networks," *IEEE Trans. Wireless Commun.*, vol. 16, no. 10, pp. 6808–6821, 2017.

[9] A. A. Boulogeorgos, P. C. Sofotasios, S. Muhaidat, M. Valkama, and G. K. Karagiannidis, "The effects of rf impairments in vehicle-to-vehicle communications," in *Proc. IEEE 26th Ann. Intl. Symp. Personal, Indoor, and Mobile Radio Commun. (PIMRC)*, 2015, pp. 840–845.

[10] Y. Xie, I. W. Ho, and E. R. Magsino, "The modeling and cross-layer optimization of 802.11p VANET unicast," *IEEE Access*, vol. 6, pp. 171–186, Oct. 2018.

[11] A. R. Ndjiongue, H. C. Ferreira, and T. M. Ngatched, "Visible light communications (VLC) technology," *Wiley Encyclopedia of Electrical and Electronics Engineering*, pp. 1–15, 1999.

[12] A. Căilean and M. Dimian, "Current challenges for visible light communications usage in vehicle applications: A survey," *IEEE Commun. Surveys Tuts*, vol. 19, no. 4, pp. 2681–2703, May. 2017.

[13] M. Uysal, Z. Ghassemlooy, A. Bekkali, A. Kadri, and H. Menouar, "Visible light communication for vehicular networking: Performance study of a V2V system using a measured headlamp beam pattern model," *IEEE Veh. Technol. Mag.*, vol. 10, no. 4, pp. 45–53, Dec. 2015.

[14] B. Turan and S. Ucar, "Vehicular visible light communications," *Visible Light Communications*, p. 133, 2017.

[15] M. Kashef, M. Ismail, M. Abdallah, K. A. Qaraqe, and E. Serpedin, "Energy efficient resource allocation for mixed RF/VLC heterogeneous wireless networks," *IEEE J. on Selected Areas in Communications*, vol. 34, no. 4, pp. 883–893, 2016.

[16] D. A. Basnayaka and H. Haas, "Hybrid RF and VLC systems: Improving user data rate performance of vlc systems," in *Proc. IEEE 81st Veh. Technol. Conf. (VTC Spring)*, 2015, pp. 1–5.

[17] X. Li, R. Zhang, and L. Hanzo, "Cooperative load balancing in hybrid visible light communications and WiFi," *IEEE Trans. Commun.*, vol. 63, no. 4, pp. 1319–1329, 2015.

[18] Y. Wang and H. Haas, "Dynamic load balancing with handover in hybrid Li-Fi and wi-fi networks," *Journal of Lightwave Technology*, vol. 33, no. 22, pp. 4671–4682, 2015.

[19] I. Stefan, H. Burchardt, and H. Haas, "Area spectral efficiency performance comparison between vlc and rf femtocell networks," in *Proc. IEEE Intl. Conf. on Communications (ICC)*, 2013, pp. 3825–3829.

[20] H. Chowdhury and M. Katz, "Cooperative data download on the move in indoor hybrid (radio-optical) wlan-vlc hotspot coverage," *Transactions on Emerging Telecommunications Technologies*, vol. 25, no. 6, pp. 666–677, 2014.

[21] M. B. Rahaim, A. M. Vegni, and T. D. C. Little, "A hybrid radio frequency and broadcast visible light communication system," in *Proc. IEEE GLOBECOM Workshops (GC Wkshps)*, 2011, pp. 792–796.

[22] H. Kazemi, M. Uysal, and F. Touati, "Outage analysis of hybrid fso/rf systems based on finite-state markov chain modeling," in *Proc. IEEE 3rd International Workshop in Optical Wireless Communications (IWOW)*, 2014, pp. 11–15.

[23] M. Haenggi, *Stochastic geometry for wireless networks*. Cambridge University Press, 2012.

[24] J. G. Andrews, F. Baccelli, and R. K. Ganti, "A tractable approach to coverage and rate in cellular networks," *IEEE Trans. Commun.*, vol. 59, no. 11, pp. 3122–3134, 2011.

[25] A. Al-Hourani and S. Kandeepan, "On modeling coverage and rate of random cellular networks under generic channel fading," *Wireless Networks*, vol. 22, no. 8, pp. 2623–2635, 2016.

[26] B. Błaszczyszyn, P. Mühlethaler, and Y. Toor, "Stochastic analysis of aloha in vehicular ad hoc networks," *Annals of telecommunications-Annales des télécommunications*, vol. 68, no. 1-2, pp. 95–106, 2013.

[27] B. Blaszczyszyn, P. Mühlethaler, and Y. Toor, "Maximizing throughput of linear vehicular ad-hoc networks (VANETs)—a stochastic approach," in *Proc. IEEE European Wireless Conference*. IEEE, 2009, pp. 32–36.

[28] Y. Jeong, J. W. Chong, H. Shin, and M. Z. Win, "Intervehicle communication: Cox-fox modeling," *IEEE J. Sel. Areas Commun.*, vol. 31, no. 9, pp. 418–433, 2013.

[29] Z. Tong, H. Lu, M. Haenggi, and C. Poellabauer, "A stochastic geometry approach to the modeling of DSRC for vehicular safety communication," *IEEE Trans. Intell. Transp. Syst.*, vol. 17, no. 5, pp. 1448–1458, 2016.

[30] B. Blaszczyszyn, P. Muhlethaler, and Y. Toor, "Performance of MAC protocols in linear VANETs under different attenuation and fading conditions," in *Proc. IEEE 12th Intl. Conf. on Intelligent Transportation Systems*, 2009, pp. 1–6.

[31] T. V. Nguyen and F. Baccelli, "A stochastic geometry model for cognitive radio networks," *The Computer Journal*, vol. 55, no. 5, pp. 534–552, 2012.

[32] E. Steinmetz, M. Wildemeersch, and H. Wymeersch, "Wip abstract: Reception probability model for vehicular ad-hoc networks in the vicinity of intersections," in *Proc. ACM/IEEE Intl. Conf. on Cyber-Physical Systems (ICCPS)*. IEEE, 2014, pp. 223–223.

[33] E. Steinmetz, R. Hult, G. R. de Campos, M. Wildemeersch, P. Falcone, and H. Wymeersch, "Communication analysis for centralized intersection crossing coordination," in *Proc. IEEE 11th International Symposium on Wireless Communications Systems (ISWCS)*. IEEE, 2014, pp. 813–818.

[34] T. Komine and M. Nakagawa, "Fundamental Analysis for Visible-Light Communication System using LED lights," *IEEE Trans. Consum. Electron.*, vol. 50, no. 1, pp. 100–107, 2004.

[35] R. B. Chiaramonte and K. R. L. J. C. Branco, "Collision detection using received signal strength in FANETs," in *Proc. IEEE International Conference on Unmanned Aircraft Systems (ICUAS)*. IEEE, 2014, pp. 1274–1283.

[36] R. C. Kizilrmak and M. Torkamani-Azar, "Reducing collision probability with multihop diversity for vehicle-to-roadside networks," in *Proc. IEEE Symposium on Wireless Technology & Applications (ISWTA)*. IEEE, 2013, pp. 17–22.

[37] S.-w. Chang, J. Cha, and S.-s. Lee, "Adaptive EDCA mechanism for vehicular ad-hoc network," in *Proc. IEEE International Conference on Information Network*. IEEE, 2012, pp. 379–383.

[38] N. Boulila and L. A. Saidane, "Medium access control in vanet," in *Proc. IEEE 6th International Conference on Communications and Networking (ComNet)*, 2017, pp. 1–6.

[39] E. Steinmetz, M. Wildemeersch, T. Q. S. Quek, and H. Wymeersch, "Packet reception probabilities in vehicular communications close to intersections," *IEEE Trans. Intell. Transp. Syst.*, pp. 1–11, 2020.

[40] B. E. Y. Belmekki, A. Hamza, and B. Escrig, "Performance analysis of cooperative communications at road intersections using stochastic geometry tools," *Digital Signal Processing*, pp. 103–112, 2021.

[41] C. A. O'cinneide, "Euler Summation for Fourier series and Laplace Transform Inversion," *Stochastic Models*, vol. 13, no. 2, pp. 315–337, 1997.

[42] J. Abate and W. Whitt, "Numerical Inversion of Laplace Transforms of Probability Distributions," *ORSA Journal on computing*, vol. 7, no. 1, pp. 36–43, 1995.

[43] A. Goldsmith, *Wireless Communications*. Cambridge university press, 2005.

[44] H.-C. Yang and M.-S. Alouini, "Wireless transmission of big data: Data-oriented performance limits and their applications," *arXiv preprint arXiv:1805.09923*, 2018.

[45] G. Singh, A. Srivastava, and V. A. Bohara, "Stochastic geometry-based interference characterization for RF and VLC-based vehicular communication system," *IEEE Syst. J.*, pp. 1–11, 2020.

[46] J. Choi, V. Marojevic, R. Nealy, J. H. Reed, and C. B. Dietrich, "DSRC and IEEE 802.11 ac adjacent channel interference assessment for the 5.9 GHz band," in *Proc. IEEE 89th VTC*, 2019, pp. 1–5.

Gurinder Singh received his Bachelor's degree (2014) from the Department of Electronics and Communication Engineering, National Institute of Technology (NIT), Meghalaya, India, and the master's degree (2016) from Indian Institute of Technology (IIT), Guwahati, India. He is currently pursuing the Ph.D. degree from Department of Electronics and Communication Engineering, IIIT-Delhi, India. He is also a Visvesvaraya Ph.D. Fellow, supported by MeitY, Government of India. His research interests include vehicular-visible light communication, Hybrid VLC-RF architecture, non-orthogonal multiple access (NOMA) and Intelligent Reflecting Surfaces (IRS) aided vehicular communication systems.

Anand Srivastava did his M.Tech. and Ph.D. (2002) from Indian Institute of Technology (IIT) Delhi, India. Before joining IIIT Delhi in 2014, he was Dean and Professor in School of Computing and Electrical Engineering at IIT Mandi, HP, India (2012-2014) and also Adjunct Professor at IIT Delhi (2008-present). Prior to this, he worked with Alcatel-Lucent- Bell Labs (2009-2012), India and Center for Development of Telematics (CDOT), a telecom research center of Govt. of India (1989-2008). During his stint in CDOT for nearly two decades, he was responsible for the development of national-level projects for Indian Telecom in the areas of Telecom Security Systems, Network Management System, Intelligent Networks, Operations Support Systems, Access Networks (GPON) and Optical Technology based products. Majority of these projects were completed successfully and commercially deployed in the public network. He also carried out significant research work in the Photonics Research Lab, Nice, France, under the Indo-French Science and Technology Cooperation Program on Special optical fibers and fiber-based components for optical communications (2007-2010). He was also closely involved with ITU-T, Geneva in Study Group 15 and represented India for various optical networking standards meetings. He has published several papers in peer-reviewed journals and conferences. He has visited Aston University, UK four times during 2014-2016 as visiting scholar under Erasmus Mundus EU program for carrying out research in optical wireless area. His current research work is in the area of optical core and access networks, fiber-wireless (FiWi) architectures, visible light communications (VLC), optical signal processing, free space optical communications and energy aware optical networks.

Vivek Ashok Bohara received the Ph.D. degree from the School of EEE, Nanyang Technological University (NTU), Singapore in 2011. From 2011 to 2013, he was a Post-Doctoral researcher (Marie Curie fellowship) in ESIEE Paris, University Paris-East. He joined IIIT-Delhi in 2013 where he is currently working as an Associate Professor. His research interests are towards next-generation communication technologies such as device-to-device communication, carrier aggregation and digital predistortion algorithms. He received 1st Prize in National Instruments ASEAN Virtual Instrumentation Applications Contest in 2007 and 2010. He was also the recipient of best poster award at IEEE ANTS 2014 and IEEE COMSNETS 2015 and 2016 conferences.

Zilong Liu received his PhD (2014) from School of Electrical and Electronic Engineering, Nanyang Technological University (NTU, Singapore), Master Degree (2007) in the Department of Electronic Engineering from Tsinghua University (China), and Bachelor Degree (2004) in the School of Electronics and Information Engineering from Huazhong University of Science and Technology (HUST, China). He is a Lecturer (Assistant Professor) at the School of Computer Science and Electronics Engineering, University of Essex. From Jan. 2018 to Nov. 2019, he was a Senior Research Fellow at the Institute for Communication Systems (ICS), Home of the 5G Innovation Centre (5GIC), University of Surrey. Prior to his career in UK, he spent nine and half years in NTU, first as a Research Associate (Jul. 2008 to Oct. 2014) and then a Research Fellow (Nov. 2014 to Dec. 2017). His PhD thesis "Perfect- and Quasi- Complementary Sequences", focusing on fundamental limits, algebraic constructions, and applications of complementary sequences in wireless communications, has settled a few long-standing open problems in the field. His research lies in the interplay of coding, signal processing, and communications, with a major objective of bridging theory and practice as much as possible. Recently, he has developed an interest in applying machine learning for wireless communications. He is a Senior Member of IEEE and an Associate Editor of IEEE Wireless Communications Letters, IEEE Access, and Frontiers in Communications and Networks. He is a General Co-Chair of the 10th International Workshop on Signal Design and its Applications in Communications (IWSDA'2022) and a TPC CoChair of the 2020 IEEE International Conference on Advanced Networks and Telecommunications Systems (ATTS'2020). Besides, he was/is a TPC member of a number of IEEE Conferences/Workshops (e.g., ICC, WCSP, GLOBECOM, ICCS, SETA, ISIT). Details of his research can be found at: https://sites.google.com/site/zilongliu2357.

Md. Noor-A-Rahim received the Ph.D. degree from Institute for Telecommunications Research, University of South Australia, Adelaide, SA, Australia, in 2015. He was a Postdoctoral Research Fellow with the Centre for Infocomm Technology, Nanyang Technological University, Singapore. He is currently a Senior Postdoctoral Researcher (MSCA Fellow) with the School of Computer Science and IT, University College Cork, Cork, Ireland. His research interests include control over wireless networks, intelligent transportation systems, information theory, signal processing, and DNA-based data storage. He was the recipient of the Michael Miller Medal from the Institute for Telecommunications Research, University of South Australia, for the most Outstanding Ph.D. Thesis in 2015.

Gourab Ghatak received the master's degree from IIT Kanpur, India, and the Ph.D. degree with a thesis on multi-RAT 5G networks from Telecom ParisTech (ENST), France, in 2019. Prior to that, he was a DAAD Research Scholar with the Vodafone Chair Mobile Communications Systems, TU Dresden, Germany, from 2014 to 2015, where he worked on channel estimation schemes for GFDM. During his Ph.D., he was employed at CEA-LETI, Grenoble. He has been an Assistant Professor with IIIT Delhi, India, since January 2019. He is the inventor of four patents and the author of several journals and conference publications. His research interests include stochastic geometry and machine learning for wireless communications. He has won the Best Paper Award from the 4th International Workshop on Smart Wireless Communications, 2017, Rome, Italy.